Synthesis, Optical, Electrochemical, and Theoretical Studies of Dipolar Ruthenium Alkynyl Complexes with Oligo(phenylenevinylene) Bridges**

Huihua Zhang,[a] Mahbod Morshedi,[b] Mahesh S. Kodikara,[b] Graeme J. Moxey,[b] Genmiao Wang,[b] Huan Wang,[a] Cristóbal Quintana,[b] Rob Stranger,[b] Chi Zhang,[a] Marie P. Cifuentes,[a,b] and Mark G. Humphrey*[a,b]

Abstract: The syntheses of oligo(*p*-phenylenevinylene)s (OPVs) end-functionalized with a ligated ruthenium alkynyl unit as a donor and a nitro as acceptor, namely *trans*-[Ru{C≡C-1-C_6H_4-4-(*E*)-CH=CH-1-C_6H_2-2,5-Et$_2$-4-(*E*)-CH=CH-1-C_6H_2-2,5-Et$_2$-4-(*E*)-CH=CH-1-C_6H_4-4-NO_2}Cl(dppe)$_2$] (**Ru4**), *trans*-[Ru{C≡C-1-C_6H_4-4-(*E*)-CH=CH-1-C_6H_2-2,5-Et$_2$-4-(*E*)-CH=CH-1-C_6H_2-2,5-Et$_2$-4-(*E*)-CH=CH-1-C_6H_2-2,5-(*n*-hexyl)$_2$-4-(*E*)-CH=CH-1-C_6H_2-2,5-(*n*-hexyl)$_2$-4-(*E*)-CH=CH-1-C_6H_4-4-NO_2}Cl(dppe)$_2$] (**Ru6**), and *trans*-[Ru{C≡C-1-C_6H_4-4-(*E*)-CH=CH-1-C_6H_2-2,5-Et$_2$-4-(*E*)-CH=CH-1-C_6H_2-2,5-Et$_2$-4-(*E*)-CH=CH-1-C_6H_2-2,5-(*n*-hexyl)$_2$-4-(*E*)-CH=CH-1-C_6H_2-2,5-(*n*-hexyl)$_2$-4-(*E*)-CH=CH-1-C_6H_2-2,5-(2-ethyl-*n*-hexyl)$_2$-4-(*E*)-CH=CH-1-C_6H_2-2,5-(2-ethyl-*n*-hexyl)$_2$-4-(*E*)-CH=CH-1-C_6H_4-4-NO_2}Cl(dppe)$_2$] (**Ru8**), are reported, together with those of precursor alkynes. Their electrochemical properties were assessed by cyclic voltammetry (CV), their linear optical and quadratic nonlinear optical (NLO) properties assayed by UV-Vis-NIR spectroscopy and hyper-Rayleigh scattering studies at 1064 nm, respectively, and their linear optical properties in the formally Ru^{III} state examined by UV-Vis-NIR spectroelectrochemistry. These data were compared to those of homologues with shorter OPV π-bridges: *trans*-[Ru(C≡C-1-C_6H_4-4-NO_2)Cl(dppe)$_2$] (**Ru1**), *trans*-[Ru{C≡C-1-C_6H_4-4-(*E*)-CH=CH-1-C_6H_4-4-NO_2}Cl(dppe)$_2$] (**Ru2**), and *trans*-[Ru{C≡C-1-C_6H_4-4-(*E*)-CH=CH-1-C_6H_4-4-(*E*)-CH=CH-1-C_6H_4-4-NO_2}Cl(dppe)$_2$] (**Ru3**). The Ru$^{II/III}$ oxidation potentials decrease on proceeding from **Ru1** to **Ru4** and then increase very slightly from **Ru4** to **Ru8**. The wavelength of the UV-Vis λ_{max} band decreases on proceeding from **Ru1** to **Ru4**, but is then essentially invariant on proceeding from **Ru4** to **Ru8**. The quadratic nonlinearity β_{1064} increases on OPV lengthening from **Ru1** through **Ru2**, reaching a maximum at **Ru3**, and then decreasing on further OPV lengthening through **Ru4**-**Ru8**. The formally Ru^{III} complexes exhibit low-energy bands at ca. 9000 cm^{-1} that red-shift slightly on proceeding from **Ru4** to **Ru8**. The effective saturation of the UV-Vis-NIR spectroscopy, HRS, and CV data is consistent with the OPV bridge in **Ru3**/**Ru4** affording the most efficient optical materials. Computational studies employing time-dependent density functional theory were undertaken on model complexes to rationalize the optical observations. The computational results are consistent with the OPV moiety acting as a bridge connecting electron donor (ligated Ru) and acceptor (NO_2) groups for the smaller complexes, with the corresponding low-energy intense transition being MLCT in nature. For the longer complexes, the connection between the termini is attenuated and the most intense transition is predominantly $\pi \rightarrow \pi^*$ in character.

Introduction

Poly(*p*-phenylenevinylene) (PPV) has been of interest for applications in light-emitting diodes (LEDs). It also possesses other technologically useful properties such as third-order optical nonlinearity and high conductivity upon doping. Mono-disperse oligo(*p*-phenylenevinylene)s (OPVs) have consequently attracted significant attention for their well-defined optical properties and thereby their potential to model aspects of PPV behavior.[1] Functionalization of OPVs by ligated metal units has been little explored until now, despite the potential materials properties advantages that this may endow (enhanced solubility, reversible redox behavior, optical properties, etc.).

The nonlinear optical (NLO) properties of molecular materials have come under considerable scrutiny. While organic molecules and polymers have been shown to possess significant optical nonlinearities, ultrafast responses, and ease of processing as films,[2] attention has also focused on organometallic complexes, which possess similar advantages as organic compounds, but with additional design flexibility (the metal, co-ligands, coordination geometry, and oxidation state can all be varied in certain cases, all leading to modification in NLO properties).[3] The most intensively studied organometallics thus far have been metallocenyl and alkynyl complexes, the latter in particular affording record values of the key NLO coefficients.[4]

[a] H. Zhang, H. Wang, Prof. C. Zhang, Prof. M. P. Cifuentes, Prof. M. G. Humphrey
School of Chemical and Material Engineering, Jiangnan University
Wuxi 214122, Jiangsu Province (P. R. China)
E-mail: mark.humphrey@jiangnan.edu.cn

[b] Dr M. Morshedi, M. S. Kodikara, Dr G. J. Moxey, Dr G. Wang, C. Quintana, Em. Prof. R. Stranger, A/Prof. M. P. Cifuentes, Prof. M. G. Humphrey
Research School of Chemistry, Australian National University, Canberra, ACT 2601 (Australia)
Fax: (+61)2-6125-0750
E-mail: mark.humphrey@anu.edu.au

[**] Part 57: Organometallic Complexes for Nonlinear Optics.

Supporting information for this article is given via a link at the end of the document.

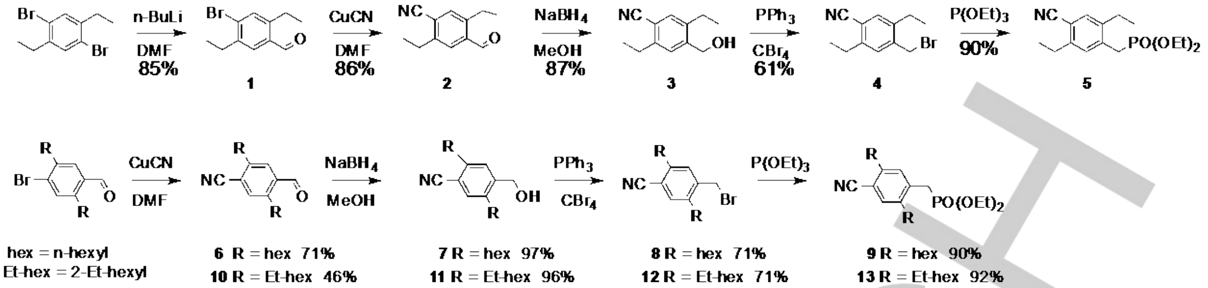

Scheme 1. Syntheses of compounds **1-13**.

Despite the strong interest in functionalized OPVs and in the NLO properties of metal alkynyl complexes, there have thus far only been limited studies of the NLO properties of stilbenes end-functionalized by (a) metal alkynyl unit(s),[5] and only one study of a similarly functionalized OPV (containing a di(phenylenevinylene) unit,[6] the shortest OPV, although octupolar and dendritic phenylenevinylene-containing complexes have been reported).[7] We report herein the syntheses of end-functionalized OPV alkynyl complexes incorporating tri-, penta-, and hepta(phenylenevinylene) groups, together with studies exploring their electrochemical and linear and quadratic nonlinear optical properties, comparisons to previously reported shorter homologues, and theoretical studies rationalizing the experimental observations.

Results and Discussion

Synthesis and characterization. OPVs end-functionalized by metal alkynyl and nitro substituents possess the donor-π-bridge-acceptor composition that can afford efficient quadratic NLO-active materials;[3] consequently, complexes with this composition were selected as targets in the present studies. The assembly of such end-functionalized OPVs necessitated the construction of organic OPVs end-functionalized by terminal alkyne and nitro groups, followed by reaction with the appropriate metal reagent. The *trans*-[RuCl(dppe)$_2$] unit was chosen as the ligated metal end-group due to its strong donor strength and because it is a key component of alkynyl complexes with reversible redox behavior, intense optical transitions, and significant NLO properties.[5l] Alkynyl complexes featuring this ligated metal combination are readily available from reaction of the five-coordinate cation [RuCl(dppe)$_2$]$^+$ with the terminal alkyne in the presence of a large non-coordinating counter-ion, followed by treatment with base.[8]

In contrast to the facile metal alkynyl complex formation, the required alkynes necessitated considerably more synthetic expense. For example, 1,4-dibromo-2,5-diethylbenzene was mono-lithiated and then reacted with DMF to form the benzaldehyde **1**, which was treated with CuCN to afford the 4-cyano-functionalized **2**. Reduction of **2** with borohydride gave **3**, which underwent an Appel reaction with CBr$_4$/PPh$_3$ to afford the bromomethyl-functionalized **4**. Reaction of **4** with P(OEt)$_3$ gave the key 4-cyanobenzylphosphonate ester building block **5.**

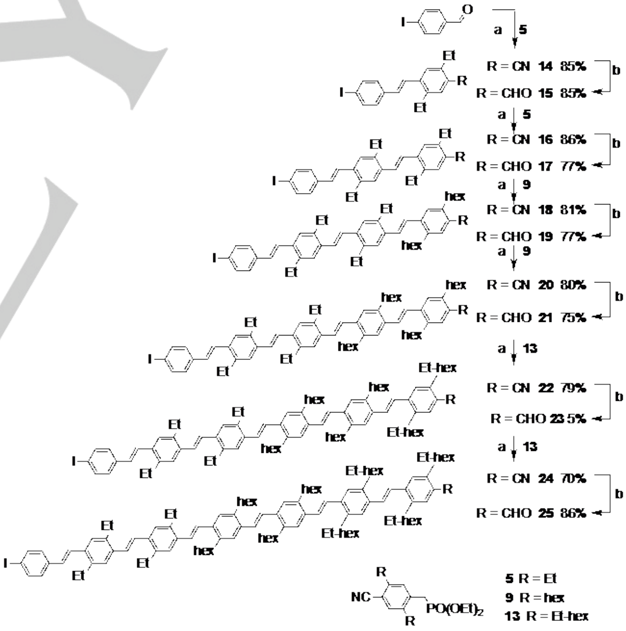

Scheme 2. Syntheses of compounds **14-25**.
Conditions: a) THF, t-BuOK, LiCl; b) DIBAL-H, toluene

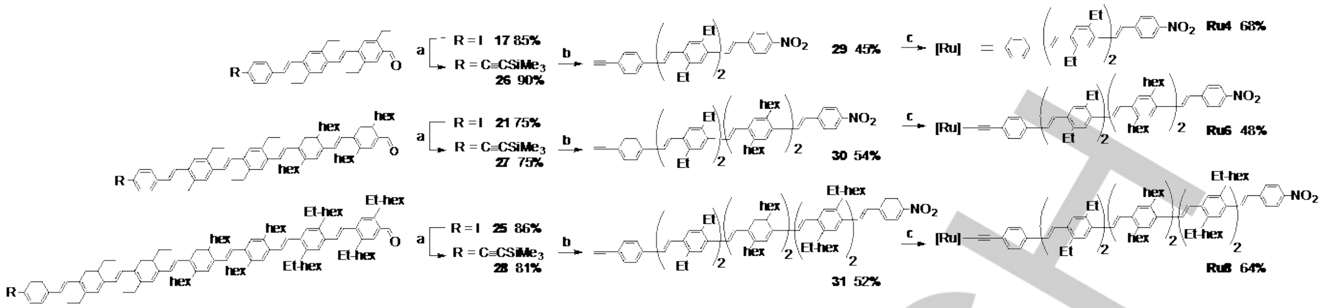

Scheme 3. Syntheses of compounds **26**-**31**, **Ru4**, **Ru6**, and **Ru8** (hex = hexyl, Et-hex = 2-ethylhexyl, [Ru] = *trans*-[RuCl(dppe)$_2$]). Conditions: a) HC≡CSiMe$_3$, PdCl$_2$(PPh$_3$)$_2$, CuI, NEt$_3$, THF; b) *p*-$O_2NC_6H_4CH_2PO(OEt)_2$, THF, t-BuOK; c) [RuCl(dppe)$_2$]PF$_6$, i. NaPF$_6$, CH$_2$Cl$_2$, ii. NEt$_3$

Initial studies revealed that the OPVs are significantly less soluble than similar-length oligo(phenyleneethynylene)s (OPEs), presumably a result of the facile rotation of the PE units in the latter, so the targeted higher OPVs in the present study necessitated the incorporation of solubilizing groups despite the potential reduction in OPV coplanarity.[1] The hexyl- and 2-ethylhexyl-functionalized compounds **9** and **13** were synthesized in a similar manner to **5** through the intermediacy of **6**-**8** and **10**-**12**, respectively (Scheme 1).

OPVs end-functionalized by iodo and aldehyde groups were then synthesized in an iterative fashion. Successive stereospecific Horner-Wadsworth-Emmons coupling of **5**, **9** and **13** with 4-iodobenzaldehyde and higher (alkyl-substituted) homologues gave a series of nitriles that were reacted with DIBAL-H in toluene to afford aldehydes following work-up (**14**-**25**, Scheme 2). Sonogashira coupling of trimethylsilylacetylene with the iodo-functionalized **17**, **21**, and **25** afforded the trimethylsilylethynyl-functionalized **26**-**28**, which were then reacted with diethyl(4-nitrobenzyl)phosphonate and potassium *tert*-butoxide in THF to give the α-alkynyl-ω-nitro-terminated OPVs **29**-**31**. Finally, the aforementioned reactions of **29**-**31** with [RuCl(dppe)$_2$]PF$_6$, followed by treatment with base, afforded the new complexes **Ru4**, **Ru6**, and **Ru8** (Scheme 3). Detailed information on synthetic procedures for **1**-**31**, **Ru4**, **Ru6**, and **Ru8** is given in the Supplementary Information.

All compounds were characterized by the usual spectroscopic and spectrometric techniques (Figures S1-S74), and the molecular structure of the oxidation product of **2** (**2-O**) as well as the molecular structures of **15**, **17**, **26**, **29** and **Ru4** were confirmed by single-crystal X-ray crystallographic studies (Figures 1 and S75-S79, Tables S1 and S2). The ^{31}P NMR spectra of the complexes **Ru4**, **Ru6**, and **Ru8** exhibit singlets at 49.5 ppm, consistent with *trans* stereochemistry at the metal centre and no effect on the dppe phosphorus chemical shift on OPV lengthening, while the IR spectra contain characteristic ν(C≡C) bands at 2050 cm^{-1}, again invariant on OPV lengthening. The identities of all three complexes were confirmed by satisfactory microanalyses and the ESI mass spectra, the latter containing molecular ions. The bond lengths and angles from the structural studies are unremarkable for the organic compounds and alkynyl complex. Of particular interest are the planarities of the OPV units. The dihedral angles along the OPV π-bridge of **Ru4** are consistent with a relatively planar arrangement from ring C3-C8 to ring C23-C28, but with the nitro-containing ring C35-C40 deviating significantly from co-planarity (Figure 1). The precursor alkyne **29** shows a similar co-planarity deviation with the nitro-functionalized ring [dihedral angles (°): C3-C8 and C11-C16: 7.123 (0.264), C11-C16 and C11'-C16': 0.000 (0.116) (due to symmetry), C11'-C16' and C3A'-C8A': 42.282 (0.481)].

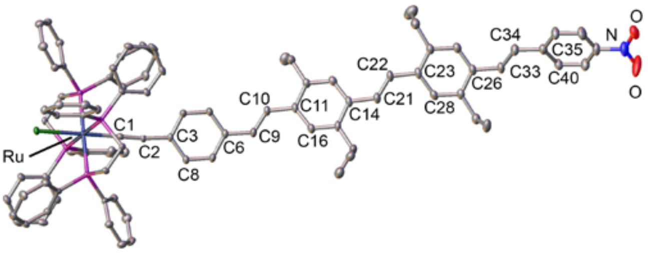

Figure 1. Molecular structure of **Ru4**, with thermal ellipsoids set at the 40% probability level. Hydrogen atoms, disordered components and the lattice dichloromethane molecule have been omitted for clarity. Selected bond lengths (Å) and angles (°): Ru1-C1 2.000(3), Ru1-P1 2.3564(8), Ru1-P2 2.3773(7), Ru1-P3 2.3835(8), Ru1-P4 2.3652(8), Ru1-Cl1 2.5085(7), C1-C2 1.216(5), P1-Ru1-Cl1 92.00(3), P1-Ru1-P2 82.07(3), P2-Ru1-Cl1 98.52(3), P3-Ru1-Cl1 82.71(3), P3-Ru1-P1 98.68(3), P3-Ru1-P2 178.55(3), P4-Ru1-Cl1 89.00(3), P4-Ru1-P1 178.98(3), P4-Ru1-P2 97.60(3), P4-Ru1-P3 81.63(3), C1-Ru1-Cl1 179.04(9), C1-Ru1-P1 88.24(9), C1-Ru1-P2 82.44(9), C1-Ru1-P3 96.34(9), C1-Ru1-P4 90.77(9). Dihedral angles (°): C3-C8 and C11-C16: 15.857(0.163), C11-C16 and C23-C28: 17.346(0.158), C23-C28 and C35-C40: 42.051(0.163).

Linear optical properties. UV-vis absorption maxima and extinction coefficients for **Ru4**-**Ru6**, together with some published data for homologues with shorter OPV π-bridges (*trans*-[Ru(C≡C-1-C_6H_4-4-NO_2)Cl(dppe)$_2$] (**Ru1**), *trans*-[Ru{C≡C-1-C_6H_4-4-(*E*)-CH=CH-1-C_6H_4-4-NO_2}Cl(dppe)$_2$] (**Ru2**), and *trans*-[Ru{C≡C-1-C_6H_4-4-(*E*)-CH=CH-1-C_6H_4-4-(*E*)-CH=CH-1-C_6H_4-4-NO_2}Cl(dppe)$_2$] (**Ru3**)), are collected in Table 1 (the spectra are provided in Figure S80). We note the varying levels of bridge alkylation across this series of complexes; alkylation of the complexes with the longer OPV π-bridges is essential on solubility grounds, and not anticipated to significantly affect the wavelength of optical absorption maximum. The low-energy optical absorption maximum red-shifts on proceeding from **Ru1** to **Ru2**, blue-shifts on proceeding from **Ru2** to **Ru3** and **Ru4**, and is then essentially invariant on further OPV lengthening to **Ru6** and **Ru8**. For **Ru1** and **Ru2**, this band corresponds to a

Table 1. Cyclic voltammetric[a] and linear optical data.[b]

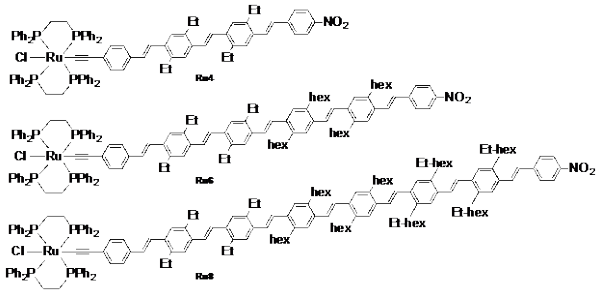

	Ru oxidation	NO_2 reduction	ν_{max} [ε] Ru^{II}	ν_{max} [ε] Ru^{III}	Ref
Ru1	0.74 [c, 0.9]	-0.84 [c, 0.8]	20 950 [2.0][d]	[c]	[5l]
Ru2	0.55 [c, 1]	-0.98 [c, 1]	20 450 [2.6][d]	[c]	[5l]
Ru3	0.54 [c, 1]	-0.91 [c, 0.9]	21 350 [1.6][d]	[c]	[6]
Ru4	0.50 [0.24; 1]	-0.99 [0.35; 0.9]	23 650 [7.7] 40 350 [6.7]	9 050 [2.3] 10 250 [1.7] 17 650 [1.7] 24 550 [6.1] 30 350 [2.9] 37 350 [5.9]	This work
Ru6	0.51 [0.12; 1]	-1.15 [0.34; 0.9]	23 350 [14.9] 30 650 [4.3] 39 850 [9.6]]	8 950 [2.7] 10 250 [2.0] 17 950 [2.4] 23 950 [12.1] 37 550 [8.0]	This work
Ru8	0.52 [0.15; 1]	-0.95 [0.52; irr]	23 550 [17.4] 30 550 [4.8] 39 450 [9.7]	8 850 [2.0] 10 150 [1.5] 18 050 [1.7] 23 850 [15.4] 39 350 [8.8]	This work

Measured in CH_2Cl_2; [a] $E_{1/2}$ (V), [ΔE (V), i_{pc}/i_{pa}], FcH/FcH$^+$ couple at 0.56 V (ΔE ≈ 0.2 V, i_{pc}/i_{pa} ≈ 1), Fc = ferrocenyl; [b] cm^{-1} [10^4 M^{-1} cm^{-1}]; [c] not reported; [d] measured in THF.

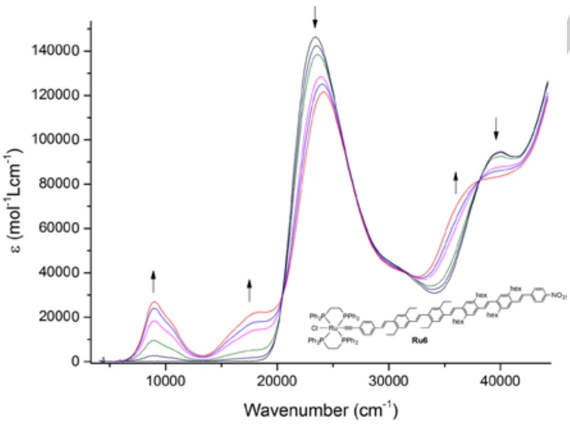

Figure 2. Progressive changes to the UV-vis spectrum for complex **Ru6** on application of a 0.7 V potential.

LUMO←HOMO MLCT transition with significant ruthenium involvement in the HOMO and nitro contribution to the LUMO;[5l,9] the λ_{max} data are suggestive of a decreasing contribution of the peripheral substituents and an increasing OPV-centred transition on OPV lengthening.

Electrochemical and spectroelectrochemical studies. The results from cyclic voltammetric studies on **Ru4**, **Ru6** and **Ru8** (Figure S81) reveal a fully reversible oxidation process for each complex at ca. 0.5 V, a potential similar to those for previously reported *trans*-[Ru(C≡CR)Cl(L_2)$_2$] complexes lacking acceptor groups (see, for example, references [5l,6,10]), together with an irreversible nitro-centred reduction at ca. -1 V (Table 1). Ruthenium complexes with 4-nitrophenylethynyl ligands show oxidation potentials of ca. 0.7 V (see **Ru1**, Table 1), reducing on π-system lengthening (see **Ru2** and **Ru3**, Table 1). The data are consistent with the longer π-bridges in the present complexes further attenuating the electron-withdrawing effect of the nitro on the ease of oxidation at the metal centre. The differences in oxidation potentials across the complexes are consistent with previous reports showing that increasing the length of the π-bridge in dipolar ruthenium alkynyl complexes with OPE bridges modifies the oxidation potential on π-system lengthening up to a tri(phenyleneethynylene) unit, the potential remaining invariant on further bridge-lengthening.[10]

In situ UV-vis spectroelectrochemical studies using an OTTLE (optically transparent thin-layer electrochemical) cell allows simultaneous collection of spectra whilst the complex is undergoing a redox process. Application of a 0.7 V potential to a sample of each complex afforded clean isosbestic points during the Ru^{II} to Ru^{III} oxidation process (Figures 2, S82 and S83), and resulted in the emergence of a new low-energy band centred at ca. 9 000 cm^{-1}, with the band shifting slightly to lower energy on chain lengthening. The fully-reversible nature of this process and the strong optical changes that accompany it are suggestive of a potential for nonlinear optical switching,[11] but we have not pursued this possibility in the present studies.

Hyper-Rayleigh scattering studies. The quadratic nonlinearities of **Ru4**, **Ru6**, and **Ru8** were determined at 1064 nm using the hyper-Rayleigh scattering technique; the results are presented in Table 2, together with the two-level corrected values. We have discussed shortcomings with the two-level model in previous reports (see, for example ref. [5l]); although the two-level model is not generally considered adequate for donor-bridge-acceptor organometallic complexes such as those in the present study, it may have some utility in cases where the structural variation is restricted to the molecular components responsible for the low-energy charge-transfer bands in the linear optical spectrum. For **Ru1** and **Ru2**, the low-energy bands for the present series of complexes are charge-transfer in nature and involve the alkynyl ligand that is the subject of systematic variation, so we have also explored the evolution of β_0 upon structural modification (while being cognizant of the aforementioned shortcomings). Table 2 also includes HRS data collected in this study for **Ru1**, **Ru2**, and **Ru3**, together with the results of previous measurements of these and related compounds. We note that, while our $\langle\beta\rangle_{HRS}$ values for **Ru2** and **Ru3** are consistent with the previously reported data (within the error margins of these measurements),

Table 2. Summary of HRS results.[a]

Complex	Structure	$\lambda_{max,}$ (nm)	$\langle\beta\rangle_{HRS}$	$\langle\beta_0\rangle$	Ref.
Ru1	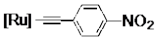	477	670 ± 170 350 ± 35 560 ± 9	105 55 88	This work [5l] [6]
Ru2	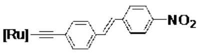	489	2310 ± 230 2700 ± 270	283 342	This work [5l]
Ru3	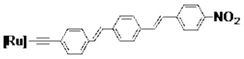	468	2570 ± 260 2525 ± 175	470 460	This work [6]
Ru4	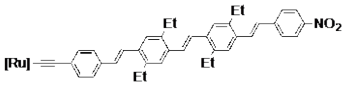	419	1355 ± 340	435	This work
Ru6	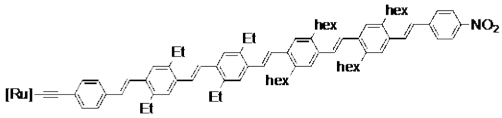	419	940 ± 240	302	This work
Ru8	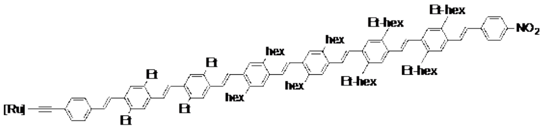	423	890 ± 220	277	This work
	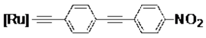	468	1240 ± 110	225	[6]
	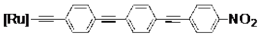	429	1327 ± 110	388	[6]
	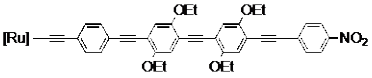	426	515 ± 50	160	[10]

[a] Measured in THF at 1064; HRS values in units of 10^{-30} esu.

our **Ru1** value differs from one of the previous reports, but is consistent with the more recent report, and close in value to that of the bis(diphenylphosphino)methane (dppm) analogue *trans*-[Ru(C≡C-1-C_6H_4-4-NO_2)Cl(dppm)$_2$] (λ_{max} = 473 nm, $\langle\beta$□$_{HRS}$ = 767 x 10^{-30} esu, $\langle\beta\rangle_0$ = 129 x 10^{-30} esu)[9].

The major focus of the present study is to assess the impact of OPV π-bridge lengthening. Proceeding from **Ru1** to **Ru2** results in a significant increase in $\langle\beta\rangle_{HRS}$ and $\langle\beta_0\rangle$ values. A smaller increase is seen on proceeding to **Ru3**. Further OPV lengthening to **Ru4** results in a decrease in these parameters, with a further reduction seen in proceeding to **Ru6** and **Ru8**. Overall, these data are consistent with a saturation effect similar to that observed with ligated-ruthenium/nitro end-functionalized OPE analogues,[10] for which nonlinearities are maximized at the same π-bridge length (Table 2). An additional important concern is to assess the relative merit of π-bridge construction via OPV or OPE units: comparison of data in Table 2 for equivalent length π-bridges reveals that the OPV-containing complexes are uniformly significantly superior to their OPE-containing analogues. The quadratic nonlinearities of the complexes in the present study are large in an absolute sense, but proximity of the charge-transfer absorption bands to the second-harmonic wavelength (532 nm) and the lack of adequacy of the two-level approximation for such compounds render further comment unwarranted; studies at longer wavelengths are needed for more detailed analysis.

Computational studies. Calculations employing density functional theory (DFT) and time-dependent DFT (TD-DFT) were undertaken to rationalize the optical properties of the complexes in the present study. Two methods (PBE1PBE and CAM-B3LYP) were used (Table S3). The diphosphine ligands of the experimental complexes were approximated by di(phosphino)methane, and varying levels of alkylation of the OPV π-bridge were explored (see below).

With TD-PBE1PBE, the calculations revealed several intense electronic transitions in the low-energy region (< 30 000 cm^{-1}) for each species; the oscillator strengths of the lowest-energy bands decrease and the intensities of the second and third lowest-energy transitions increase with increasing OPV π-bridge length (Table S4). Furthermore, the second-lowest-energy transition, particularly for the longer species (i.e. the $S_0 \rightarrow S_2$ transition for models of complexes longer than **Ru4**), dominates the electronic transitions in the lower-energy region. In contrast, CAM-B3LYP predicted only one transition with a large oscillator strength in the same region. The calculated intensity of this red-shifting transition shows a gradual increase with increasing π-bridge length and so, as a result, the TD-CAM-B3LYP calculations suggest an intense narrow band, particularly for the larger complexes, in the lower-energy region of the UV-Vis spectrum. All of these singlet-excited transitions (apart from the $S_0 \rightarrow S_1$ calculated by TD-PBE1PBE) are associated with multiple single-electron transitions between several occupied and unoccupied frontier molecular orbitals. Natural transition orbitals (NTOs)[12] were therefore calculated as an alternative way to describe the character of the transitions in the current work.

Figures S84 and S85 display the calculated NTOs using PBE1PBE and CAM-B3LYP, respectively. The NTOs in Figure S84 reveal that the intense lowest-energy transition is predominately metal-to-ligand charge transfer (MLCT) with other transitions showing admixture of MLCT and intra-ligand CT character (ILCT: $\pi \rightarrow \pi^*$ within the phenylenevinylene unit). Moreover, it appears that the ILCT contribution, particularly to the second-lowest-energy transition, grows gradually and the strong overlap within the hole-particle pair, particularly for the longer system, seems to result in an increase in transition dipole moment (oscillator strength) for this transition.

Figure S85 shows the NTOs calculated with CAM-B3LYP. These results indicate that, particularly for the smaller complexes, the OPV moiety mainly functions as a bridge interconnecting electron donor (Ru) and acceptor (NO_2) groups. For the larger complexes **Ru6** through **Ru8**, the most intense transition is predominantly $\pi \rightarrow \pi^*$ in character. On the basis of these results, we conclude that the OPV unit has the dual role of acting as a bridge (when the number of repeat units n is small) and acting as a donor-acceptor pair (when n is large), as shown by a deterioration of the donor (metal) – acceptor (nitro) interaction in the larger complexes.

Calculations were also undertaken on several complexes with methylated spacers (**Ru4"**, **Ru6"**, and **Ru8"**). These model species were built by methylation of the non-nitro-containing phenylene groups in the OPV unit of the corresponding model complex (i.e. **Ru4'**, **Ru6'**, and **Ru8'**). All these compounds were constrained to C_s symmetry. Methyl groups were used as small analogues of the ethyl, hexyl, and 2-ethylhexyl substituents used in the experimental studies. The calculated UV-Vis results (Table S4) do not show significant differences between **Ru4"** and **Ru4'"**. Furthermore, the calculated UV-Vis spectrum of **Ru6"** nicely reproduces that of **Ru6'"**; thus, methyl is an effective model for the larger alkyl substituents that were used to overcome solubility problems. Next, the UV-Vis spectra of methylated **Ru4"**, **Ru6"**, and **Ru8"** were compared with their “unadorned” analogues **Ru4'**, **Ru6'**, and **Ru8'**, respectively (see Table S4). Although methylation has a minor effect, a slight blue shift in the intense low-energy transitions can be seen when methyl substituents are introduced. In TD-PBE1PBE calculations on **Ru6"** and **Ru8"**, an additional electronic transition is seen in the low-energy region but its intensity is very small compared with the most intense transition. Overall, alkylation has a minor effect on linear optical data.

All of the calculations summarized thus far were undertaken on complexes with planar OPV bridges. With both DFT functionals employed, the calculations revealed that increasing π-bridge length resulted in the lowest energy transition moving to longer wavelength, but the empirical data are inconsistent with this. For example, the experimental absorption maxima of **Ru4**, **Ru6**, and **Ru8** exist in a narrow spectral region (23 500 cm^{-1} – 24 000 cm^{-1}) and they are significantly blue-shifted compared to the bands in the UV-Vis spectra of shorter compounds. Similarly, a blue-shift in the lowest-energy band is seen on proceeding from **Ru2**[5l] to **Ru3**.[6] The C_s point group imposed during the aforementioned calculations does not allow the π-bridge phenyl groups to alter the idealized coplanar arrangement, and thus this may not represent the statistically averaged structures pertaining under laboratory conditions. Moreover, the large alkyl groups used experimentally to overcome solubility problems may also have a substantial effect on phenyl orientation. For these reasons, the effect of ring torsion in **Ru3'** was investigated by rotating the terminal phenyl group with respect to the rest of the π-bridge. (Note that we have tested only the terminal alkenyl-aryl bond rotation in order to simplify the analysis, but this is a realistic initial approach, and indeed this corresponds to the ring exhibiting significant deviation from co-planarity in the structural studies of **Ru4** and **29**: see above.) First, geometrical structures were optimized as a function of the angle (θ) between the terminal phenyl group and the alkenyl linkage. Next, UV-Vis calculations on the optimized, angle-constrained geometries were undertaken. Low-lying transitions with large oscillator strengths for each conformation are summarized in Table S5. Not surprisingly, deviating from an ideal coplanar arrangement ($\theta = 0°$), possessing very strong π-conjugation, to an orthogonal conformation ($\theta = 90°$) results in a gradual increase in total energy as conjugation breaks at the orthogonal junction. However, for angles θ up to 40°- 45°, the rotational energy barrier is relatively small. Consequently, the experimental complex **3**, the laboratory analogue of the theoretical construct **Ru3'**, is expected to exist in a relatively broad range of torsional conformations, particularly in solution. Calculated TD-DFT results indicate that twisting of the terminal 4-nitrophenyl group from $\theta = 0°$ to 90° results in a blue-shift and a gradual increase in intensity of the lowest energy band (Table S5). Since opportunities for twisting phenyl/phenylene groups are increased as the OPV unit increases in length, it is possible that the experimental observation of a blue-shift in the lowest-energy absorption band may result from this spectral band comprising several overlapping transitions given by conformations with both planar and non-planar phenylenevinylene moieties. Nevertheless, as Table S4 indicates, particularly for the larger complexes, further increasing the OPV length has little influence on the band position, and this behaviour, along with rotations within the OPV, may be extrapolated to interpret the laboratory observation of absorption maxima for **Ru4**, **Ru6**, and **Ru8**.

Conclusions

In combination with previously reported shorter homologues, the complexes **Ru4**, **Ru6**, and **Ru8** comprise a set of end-functionalized OPV-containing dipolar organometallics. These complexes have afforded the opportunity to explore the effect of bridge variation on electrochemical and optical properties. The $Ru^{II/III}$ oxidation potentials decrease on proceeding from **Ru1** to **Ru4** and then increase very slightly on proceeding from **Ru4** to **Ru8**, the wavelength of the UV-vis λ_{max} band decreases on proceeding from **Ru1** to **Ru4**, but is then essentially invariant on proceeding from **Ru4** to **Ru8**, and the quadratic nonlinearity β_{1064} increases on OPV lengthening from **Ru1** through **Ru2**, reaches a maximum at **Ru3**, and decreases on further OPV lengthening through **Ru4**-**Ru8**. These data are all consistent with an effective conjugation length consisting of a tri(phenylenevinylene) unit. Beyond this bridge length, properties plateau or are maximized. Similar observations have been noted with other ruthenium complexes. The evolution in linear and quadratic NLO properties of tetrakis(ammine)ruthenium complexes bearing 4-vinylpyridine ligands [*trans*-[Ru(1-NC$_5$H$_4$-4-{(*E*)-CH=CH}$_n$-1-C$_5$H$_4$NMe-4)(L)(NH$_3$)$_4$](PF$_6$)$_3$ (L = *N*-methylimidazole, pyridine, NH$_3$; n = 0-3) has been explored; the lowest-energy bands blue-shift as the number of *E*-ene groups increases and the static first hyperpolarizability β_0 peaks at n = 2, results ascribed to increasing π-character of the HOMO (and thereby decreasing MLCT character and increasing ILCT character of the lowest-energy transition) on increasing the conjugation length.[13] The evolution of linear, quadratic, and cubic NLO properties of *trans*-[Ru(C≡C-{1-C$_6$H$_4$-4-C≡C-}$_n$1-C$_6$H$_4$-4-NO$_2$)Cl(dppm)$_2$] (n = 0-2) and *trans*-[Ru(C≡C-{1-C$_6$H$_4$-4-C≡C-}$_2${1-C$_6$H$_2$-2,5-(OEt)$_2$-4-C≡C}$_n$1-C$_6$H$_4$-4-NO$_2$)Cl(dppm)$_2$] (n = 1, 2) has also been explored; the lowest-energy bands blue-shift as the number of phenyleneethynylene units increases, plateauing at the tri(phenyleneethynylene) complex, and the quadratic and cubic NLO properties peak at the same conjugation length, an outcome ascribed to decreasing LUMO ← HOMO transition importance and increasing on-axis aryl rotation-mediated change in relative intensities of key close-lying transitions.[10] In the present case, the computational studies suggest that similar intra-OPV rotations, and a consequent plethora of conformational possibilities, results in the experimentally observed relatively invariant optical properties.

The quadratic nonlinearities for the present complexes are large, although the proximity of the optical absorption maxima to the laser second-harmonic wavelength is consistent with significant resonance enhancement. The two-level corrected nonlinearities are very large for complexes of this size, but the model on which these calculations are based is probably inapplicable for such complexes. Nevertheless, while being mindful of these considerations, comparisons within the series of closely related complexes are useful. One clear trend is to confirm that the observation with organic systems of the increased efficacy of phenylenevinylene vs phenyleneethynylene-based bridges is maintained on proceeding to metal alkynyl complexes. The present studies have also defined **Ru3** as possessing the specific OPV π-bridge length to afford the most efficient optical material with this ligated-metal unit as donor group, a similar outcome to that seen with end-functionalized OPE analogues (see above). Finally, the experimental observations and the calculations suggest that while end-functionalization can certainly modulate OPV properties, this does not necessarily preclude a negative impact on π-system co-planarity.

Acknowledgements

We thank the Australian Research Council (ARC), the National Natural Science Foundation of China (51432006), the Chinese Government Ministry of Education, and the Chinese Government State Administration of Foreign Experts Affairs (111 Project: B13025). M.P.C. thanks the ARC for an Australian Research Fellowship and C.Q. thanks CONICYT (Chile) for a Chile PhD Scholarship Abroad.

Keywords

Organometallic chemistry • Molecular electrochemistry • Nonlinear optics • Transition metals

Supporting Information

Complete details of the syntheses and characterization of compounds **1**-**31**, and complexes **Ru4**, **Ru6**, and **Ru8**, crystallographic studies of **2-O**, **15**, **17**, **26**, **29**, and **Ru4**, cyclic voltammetric and UV-vis-NIR spectroelectrochemical studies of all new complexes, hyper-Rayleigh scattering studies at 1064 nm of **Ru1**, **Ru2**, **Ru3**, **Ru4**, **Ru6**, and **Ru8**, and theoretical studies of models of **Ru2**-**Ru8** are reported in the Supporting Information, available on the WWW under http://dx.doi.org/10.1002/chem.2016xxxxx.

References

[1] M. S. Wong, M. Samoc, A. Samoc, B. Luther-Davies, M. G. Humphrey, *J. Mater. Chem.* **1998**, *8*, 2005-2009.

[2] See, for example: a) D. J. Williams, Ed., in *Nonlinear Optical Properties of Organic and Polymeric Materials*, *ACS Symposium Series, Vol. 233*, ACS, Washington, D.C., **1983**; b) D. S. Chemla, J. Zyss, Eds., *Nonlinear Optical Properties of Organic Molecules and Crystals I*, Academic Press, Orlando, **1987**; c) D. S. Chemla, J. Zyss, Eds., *Nonlinear Optical Properties of Organic Molecules and Crystals II*, Academic Press, Orlando, **1987**; d) A. J. Heeger, J. Orenstein, D. R. Ulrich, Eds., *Nonlinear Optical Properties of Polymers*, Materials Research Society, Pittsburgh, **1988**; e) R. A. Hann, D. Bloor, Eds., *Organic Materials for Non-linear Optics*, Royal Society of Chemistry, London, **1989**; f) M. H. Lyons, Ed., *Materials for Non-linear and Electro-optics 1989*, Institute of Physics, Bristol, **1989**; g) S. R. Marder, J. W. Perry, W. P. Schaefer, E. J. Ginsburg, C. B. Gorman, R. H. Grubbs, *Mat. Res. Soc. Symp. Proc.* **1990**, *175*, 101-106.

[3] a) J. P. L. Morrall, G. T. Dalton, M. G. Humphrey, M. Samoc, *Adv. Organomet. Chem.* **2007**, *55*, 61-136; b) M. G. Humphrey, T. Schwich, P. J. West, M. P. Cifuentes, M. Samoc, in *Comprehensive Inorganic Chemistry II, Vol. 8* (Eds.: J. Reedijk, K. Poeppelmeier), Elsevier, Oxford, UK, **2013**, pp. 781-835; c) K. A. Green, M. P. Cifuentes, M. Samoc, M. G. Humphrey, *Coord. Chem. Rev.* **2011**, *255*, 2530-2541; d) B. J. Coe, in *Comprehensive Coordination Chemistry II, Vol. 9* (Eds.: J. A. McCleverty, T. J. Meyer), Elsevier, Oxford, UK, **2004**, pp. 621-687; e) M. E. Thompson, P. E. Djurovich, S. Barlow, S. Marder, in *Comprehensive Organometallic Chemistry III, Vol. 12* (Eds.: R. H. Crabtree, D. M. P. Mingos), Elsevier, Oxford, UK, **2007**, pp. 101-194; f) C. Andraud, O. Maury, *Eur. J. Inorg. Chem.* **2009**, 4357-4371.

[4] a) P. V. Simpson, L. A. Watson, A. Barlow, G. Wang, M. P. Cifuentes, M. G. Humphrey, *Angew. Chem. Int. Ed.* **2016**, *55*, 2387-2391; b) A. M. McDonagh, M. P. Cifuentes, M. G. Humphrey, S. Houbrechts, J. Maes, A. Persoons, M. Samoc, B. Luther-Davies, *J. Organomet. Chem.* **2000**, *610*, 71-79.

[5] a) I. R. Whittall, M. G. Humphrey, M. Samoc, J. Swiatkiewicz, B. Luther-Davies, *Organometallics* **1995**, *14*, 5493-5495; b) A. M. McDonagh, M. P. Cifuentes, I. R. Whittall, M. G. Humphrey, M. Samoc, B. Luther-Davies, D. C. R. Hockless, *J. Organomet. Chem.* **1996**, *526*, 99-103; c) A. M.

McDonagh, I. R. Whittall, M. G. Humphrey, D. C. R. Hockless, B. W. Skelton, A. H. White, *J. Organomet. Chem* **1996**, *523*, 33-40; d) A. M. McDonagh, I. R. Whittall, M. G. Humphrey, B. W. Skelton, A. H. White, *J. Organomet. Chem.* **1996**, *519*, 229-235; e) I. R. Whittall, M. G. Humphrey, S. Houbrechts, A. Persoons, D. C. R. Hockless, *Organometallics* **1996**, *15*, 5738; f) I. R. Whittall, M. G. Humphrey, A. Persoons, S. Houbrechts, *Organometallics* **1996**, *15*, 1935-1941; g) I. R. Whittall, M. P. Cifuentes, M. G. Humphrey, B. Luther-Davies, M. Samoc, S. Houbrechts, A. Persoons, G. A. Heath, D. Bogsanyi, *Organometallics* **1997**, *16*, 2631-2637; h) I. R. Whittall, M. P. Cifuentes, M. G. Humphrey, B. Luther-Davies, M. Samoc, S. Houbrechts, A. Persoons, G. A. Heath, D. C. R. Hockless, *J. Organomet. Chem.* **1997**, *549*, 127-137; i) I. R. Whittall, M. G. Humphrey, M. Samoc, B. Luther-Davies, D. C. R. Hockless, *J. Organomet. Chem.* **1997**, *544*, 189-196; j) I. R. Whittall, M. G. Humphrey, M. Samoc, B. Luther-Davies., *Angew. Chem. Int. Ed. Engl.* **1997**, *36*, 370-371; k) J. Vicente, M. T. Chicote, M. D. Abrisqueta, M. C. Ramîrez de Arellano, P. G. Jones, M. G. Humphrey, M. P. Cifuentes, M. Samoc, B. Luther-Davies, *Organometallics* **2000**, *19*, 2968-2974; l) S. Hurst, M. P. Cifuentes, J. P. L. Morrall, N. T. Lucas, I. R. Whittall, M. G. Humphrey, I. Asselberghs, A. Persoons, M. Samoc, B. Luther-Davies, A. C. Willis, *Organometallics* **2001**, *20*, 4664-4675; m) J. P. Morrall, M. P. Cifuentes, M. G. Humphrey, R. Kellens, E. Robijns, I. Asselberghs, K. Clays, A. Persoons, M. Samoc, A. C. Willis, *Inorg. Chim. Acta* **2006**, *359*, 998-1005; n) M. H. Garcia, M. P. Robalo, A. R. Dias, M. T. Duarte, W. Wenseleers, G. Aerts, E. Goovaerts, M. P. Cifuentes, S. Hurst, M. G. Humphrey, M. Samoc, B. Luther-Davies, *Organometallics* **2002**, *21*, 2107-2118; o) F. Nisic, A. Colombo, C. Dragonetti, E. Garoni, D. Marinotto, S. Righetto, F. De Angelis, M. G. Lobello, P. Salvatori, P. Biagini, F. Melchiorre, *Organometallics* **2015**, *34*, 94-104.

[6] L. Rigamonti, B. Babgi, M. P. Cifuentes, R. L. Roberts, S. Petrie, R. Stranger, S. Righetto, A. Teshome, I. Asselberghs, K. Clays, M. G. Humphrey, *Inorg. Chem.* **2009**, *48*, 3562-3572.

[7] a) S. K. Hurst, M. G. Humphrey, T. Isoshima, K. Wostyn, I. Asselberghs, K. Clays, A. Persoons, M. Samoc, B. Luther-Davies, *Organometallics* **2002**, *21*, 2024-2026; b) S. K. Hurst, N. T. Lucas, M. G. Humphrey, T. Isoshima, K. Wostyn, I. Asselberghs, K. Clays, A. Persoons, M. Samoc, B. Luther-Davies, *Inorg. Chim. Acta* **2003**, *350*, 62-76; c) C. J. Jeffery, M. P. Cifuentes, G. T. Dalton, T. C. Corkery, M. D. Randles, A. C. Willis, M. Samoc, M. G. Humphrey, *Macromol. Rapid Commun.* **2010**, *31*, 846-849; d) Z. Chen, C. J. Jeffery, M. Morshedi, G. J. Moxey, A. Barlow, X. Yang, B. A. Babgi, G. T. Dalton, M. D. Randles, M. K. Smith, C. Zhang, M. Samoc, M. P. Cifuentes, M. G. Humphrey, *ChemPlusChem* **2015**, *80*, 1329-1340.

[8] a) N. Gauthier, N. Tchouar, F. Justaud, G. Argouarch, M. P. Cifuentes, L. Toupet, D. Touchard, J.-F. Halet, S. Rigaut, M. G. Humphrey, K. Costuas, F. Paul, *Organometallics* **2009**, *28*, 2253-2266; b) G. Grelaud, M. P. Cifuentes, T. Schwich, G. Argouarch, S. Petrie, R. Stranger, F. Paul, M. G. Humphrey, *Eur. J. Inorg. Chem.* **2012**, 65-75; c) S. Marques-Gonzalez, D. S. Yufit, J. A. K. Howard, M. Kaupp, P. J. Low, *Organometallics* **2014**, *33*, 4947-4963.

[9] R. H. Naulty, A. M. McDonagh, I. R. Whittall, M. P. Cifuentes, M. G. Humphrey, S. Houbrechts, J. Maes, A. Persoons, G. A. Heath, D. C. R. Hockless, *J. Organomet. Chem.* **1998**, *563*, 137-146.

[10] B. Babgi, L. Rigamonti, M. P. Cifuentes, T. C. Corkery, M. D. Randles, T. Schwich, S. Petrie, R. Stranger, A. Teshome, I. Asselberghs, K. Clays, M. Samoc, M. G. Humphrey, *J. Am. Chem. Soc.* **2009**, *131*, 10293-10307.

[11] Redox-switching of the NLO properties of Ru^{II} alkynyl complexes: a) K. A. Green, M. P. Cifuentes, T. C. Corkery, M. Samoc, M. G. Humphrey, *Angew. Chem. Int. Ed.* **2009**, *48*, 7867-7870; b) G. T. Dalton, M. P. Cifuentes, S. Petrie, R. Stranger, M. G. Humphrey, M. Samoc, *J. Am. Chem. Soc.* **2007**, *129*, 11882-11883; c) M. P. Cifuentes, C. E. Powell, J. P. Morrall, A. M. McDonagh, N. T. Lucas, M. G. Humphrey, M. Samoc, S. Houbrechts, I. Asselberghs, K. Clays, A. Persoons, T. Isoshima, *J. Am. Chem. Soc.* **2006**, *126*, 10819-10832; d) C. E. Powell, M. G. Humphrey, M. P. Cifuentes, J. P. Morrall, M. Samoc, B. Luther-Davies, *J. Phys. Chem. A* **2003**, *107*, 11264-11266; e) C. E. Powell, M. P. Cifuentes, J. P. L. Morrall, R. Stranger, M. G. Humphrey, M. Samoc, B. Luther-Davies, G. A. Heath, *J. Am. Chem. Soc.* **2003**, *125*, 602-610; f) M. P. Cifuentes, C. E. Powell, M. G. Humphrey, G. A. Heath, M. Samoc, B. Luther-Davies, *J. Phys. Chem. A* **2001**, *105*, 9625 - 9627; Redox-switching of the NLO properties of other compounds: g) B. J. Coe, S. Houbrechts, I. Asselberghs, A. Persoons, *Angew. Chem. Int. Ed.* **1999**, *38*, 366-369; h) T. Weyland, I. Ledoux, S. Brasselet, J. Zyss, C. Lapinte, *Organometallics* **2000**, *19*, 5235-5237; i) M. Malaun, R. L. Paul, J. C. Jeffery, J. A. McCleverty, M. D. Ward, I. Asselberghs, K. Clays, A. Persoons, *Chem. Commun.* **2001**, 49-50; j) F. Paul, K. Costuas, I. Ledoux, S. Deveau, J. Zyss, J.-F. Halet, C. Lapinte, *Organometallics* **2002**, *21*, 5229-5235; k) B. J. Coe, N. R. M. Curati, *Comments Inorg. Chem.* **2004**, *25*, 147-184; l) I. Asselberghs, K. Clays, A. Persoons, A. M. McDonagh, M. D. Ward, J. A. McCleverty, *Chem. Phys. Lett.* **2003**, *368*, 408-411.

[12] R. L. Martin, *J. Chem. Phys.* **2003**, *118*, 4775-4777.

[13] a) B. J. Coe, L. A. Jones, J. A. Harris, B. S. Brunschwig, I. Asselberghs, K. Clays, A. Persoons, *J. Am. Chem. Soc.* **2003**, *125*, 862-863; b) B. J. Coe, L. A. Jones, J. A. Harris, B. S. Brunschwig, I. Asselberghs, K. Clays, A. Persoons, J. Garin, J. Orduna, *J. Am. Chem. Soc.* **2004**, *125*, 3880-3891.

Entry for the Table of Contents

FULL PAPER

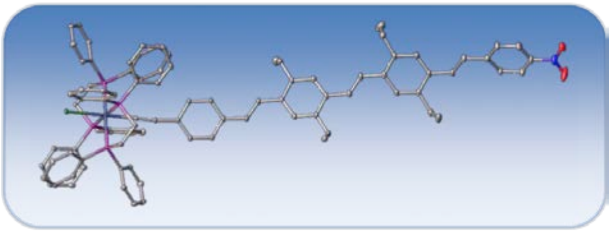

For end-functionalized OPVs with a donor ligated ruthenium centre and acceptor nitro group, oxidation potentials and wavelength of the UV-Vis λ_{max} band plateau and quadratic nonlinearities are maximized around the complex with a tri(phenylenevinylene) unit. Computational studies suggest that intra-OPV rotations result in the experimentally observed relatively invariant properties for the higher OPV examples.

*Huihua Zhang, Mahbod Morshedi, Mahesh S. Kodikara, Graeme J. Moxey, Genmiao Wang, Huan Wang, Cristóbal Quintana, Rob Stranger, Chi Zhang, Marie P. Cifuentes, and Mark G. Humphrey**

Page No. – Page No.

Synthesis, Optical, Electrochemical, and Theoretical Studies of Dipolar Ruthenium Alkynyl Complexes with Oligo(phenylenevinylene) Bridges